

Lightweight 3D LiDAR-Based UAV Tracking: An Adaptive Extended Kalman Filtering Approach*

Nivand Khosravi¹ , Meysam Basiri¹ , and Rodrigo Ventura¹ 

Institute for Systems and Robotics (ISR), Instituto Superior Técnico, Lisbon,
Portugal
{nivand.khosravi, meysam.basiri, rodrigo.ventura}@tecnico.ulisboa.pt

Abstract. Accurate relative positioning is crucial for swarm aerial robotics, enabling coordinated flight and collision avoidance. While vision-based tracking has been extensively studied, 3D LiDAR-based methods remain underutilized, despite their robustness in varying lighting conditions. Existing systems often rely on bulky, power-intensive sensors, making them impractical for small UAVs with strict payload and energy constraints. This paper presents a lightweight LiDAR-based UAV tracking system incorporating an Adaptive Extended Kalman Filtering (AEKF) framework. Our approach effectively handles the challenges posed by sparse, noisy, and nonuniform point cloud data generated by non-repetitive scanning 3D LiDARs, ensuring reliable tracking while remaining suitable for small drones with strict payload constraints. Unlike conventional filtering techniques, the proposed method dynamically adjusts noise covariance matrices using innovation and residual statistics, enhancing the tracking accuracy under real-world conditions. Additionally, a recovery mechanism ensures continuity of tracking during temporary detection failures caused by scattered LiDAR returns or occlusions.

Experimental validation using a Livox Mid-360 LiDAR on a DJI F550 UAV demonstrates successful UAV tracking in real-world conditions, overcoming sparse returns and intermittent detection while outperforming standard Kalman filter-based motion tracking during challenging maneuvers. To the best of our knowledge, this is the first adaptive noise covariance estimation framework applied to UAV-to-UAV relative tracking using a non-repetitive scanning LiDAR on a payload-constrained airborne platform. Results confirm our framework enables reliable relative positioning in GPS-denied environments without multi-sensor arrays or ground infrastructure.

Keywords: UAV Tracking · Adaptive Kalman Filter · 3D LiDAR-Based Tracking.

* Accepted at the 19th International Conference on Intelligent Autonomous Systems (IAS-19). To be published in Intelligent Autonomous Systems 19 Proceedings of IAS-19, Volume 2, in Networks and Systems, Springer Nature. This is the authors' preprint version; the final authenticated publication will be available via Springer.

1 Introduction

The ability to reliably detect and track small UAVs is crucial in various scenarios, including swarm coordination, autonomous interception, and airspace management [1, 2]. This task becomes particularly challenging in GPS-denied or restricted environments, such as indoor spaces, urban canyons, dense foliage, or areas affected by electromagnetic interference, where absolute positioning is unreliable. In such scenarios, UAVs must rely on onboard sensors to track cooperative and non-cooperative aerial agents for safe navigation and effective coordination. Consequently, robust relative positioning and tracking are critical for mission-critical applications, including search and rescue, surveillance, and autonomous drone delivery [3].

Vision-based tracking systems utilizing deep learning models, such as YOLO with SORT or Siamese networks, perform well under optimal conditions [2, 4]. However, these methods are significantly degraded in environments with low light, poor visibility, or adverse weather conditions [1, 5]. LiDAR-based sensing presents a viable alternative by providing three-dimensional measurements that are independent of lighting conditions [6, 7]. Despite this advantage, LiDAR-based UAV tracking remains challenging, particularly when tracking small agile drones with minimal reflective surfaces. Commonly used tracking methods exhibit limitations in this context. Vision-based systems often exceed the computational capacity of lightweight UAV platforms, while standard LiDAR trackers struggle with sparse point cloud data from small UAVs. Multisensor fusion techniques, although effective, introduce additional processing overhead, calibration complexities, and system integration challenges, which may conflict with the strict payload and energy constraints of small aerial platforms [8].

Modern compact LiDAR sensors, such as the Livox Mid-360, utilize non-repetitive scanning patterns that generate fundamentally different data characteristics compared to traditional LiDAR systems. These scanning patterns result in irregular point distributions, significant density variations, and inconsistent feature visibility between frames [9, 10]. Existing tracking algorithms, which assume uniform scanning patterns and consistent measurement quality, are incompatible with processing such data, necessitating the development of novel tracking approaches tailored to these unique sensor characteristics.

This paper presents a robust LiDAR-based tracking framework designed to address these challenges. Our approach focuses on effectively processing non-repetitive pattern point cloud data for relative localization between small UAVs. Our key contributions are as follows.

1. **Adaptive Filtering for Variable Data Quality:** A filtering method that dynamically adjusts noise parameters based on the reliability assessment of real-time measurement, addressing the inherent variations in non-repetitive scanning data.
2. **Robust Data Association in Irregular Point Clouds:** Mahalanobis distance-based validation gating to manage uncertainties in non-uniform point clouds, ensuring continuous tracking even in cluttered environments.

3. **Recovery Mechanism for Intermittent Detections:** A specialized strategy that maintains tracking continuity during measurement gaps by smoothly reinitializing tracking after temporary occlusions or target excursions beyond sensor range.
4. **Optimized Clustering for Sparse Data:** An optimized DBSCAN clustering algorithm tuned for sparse LiDAR returns, facilitating precise UAV segmentation without secondary sensor modalities.

Comprehensive validation in relative positioning scenarios between small UAVs demonstrates that our framework achieves accurate, reliable tracking without dependence on absolute coordinate systems, addressing a critical gap in UAV tracking technology for autonomous operations in GPS-denied environments.

The remainder of this paper is structured as follows. Section 2 presents an overview of the complete system architecture. Section 3 reviews existing LiDAR-based UAV tracking methodologies. Section 4 details our adaptive Kalman filtering framework. Section 5 presents experimental results. Finally, Section 6 concludes with key findings and future directions.

2 System Overview

Figure 1 presents the complete architecture of our LiDAR-based UAV tracking system. The pipeline is organized into three interconnected stages: (i) point cloud processing and DBSCAN-based cluster extraction, (ii) data association with Mahalanobis gating and recovery logic, and (iii) the Adaptive Extended Kalman Filter with online noise covariance tuning. Raw scans from the Livox Mid-360 enter Stage I, where voxel downsampling, cylindrical ROI filtering, and DBSCAN produce candidate drone clusters. These clusters feed Stage II, where they are matched against the filter’s predicted state via Mahalanobis distance gating; unmatched frames trigger the recovery module. Validated measurements are finally consumed by Stage III, where the constant-acceleration EKF propagates the target state and simultaneously refines both Q_k and R_k from the innovation and residual statistics.

3 Related Work

UAV tracking has been pursued using various sensor modalities, with vision-based and LiDAR-based systems representing the primary approaches. These methods differ in detection principles, environmental resilience, computational demands, and tracking precision.

3.1 LiDAR-Based UAV Tracking

LiDAR-based tracking overcomes many limitations of vision-based systems in challenging conditions such as poor lighting or adverse weather [6, 10, 11]. By

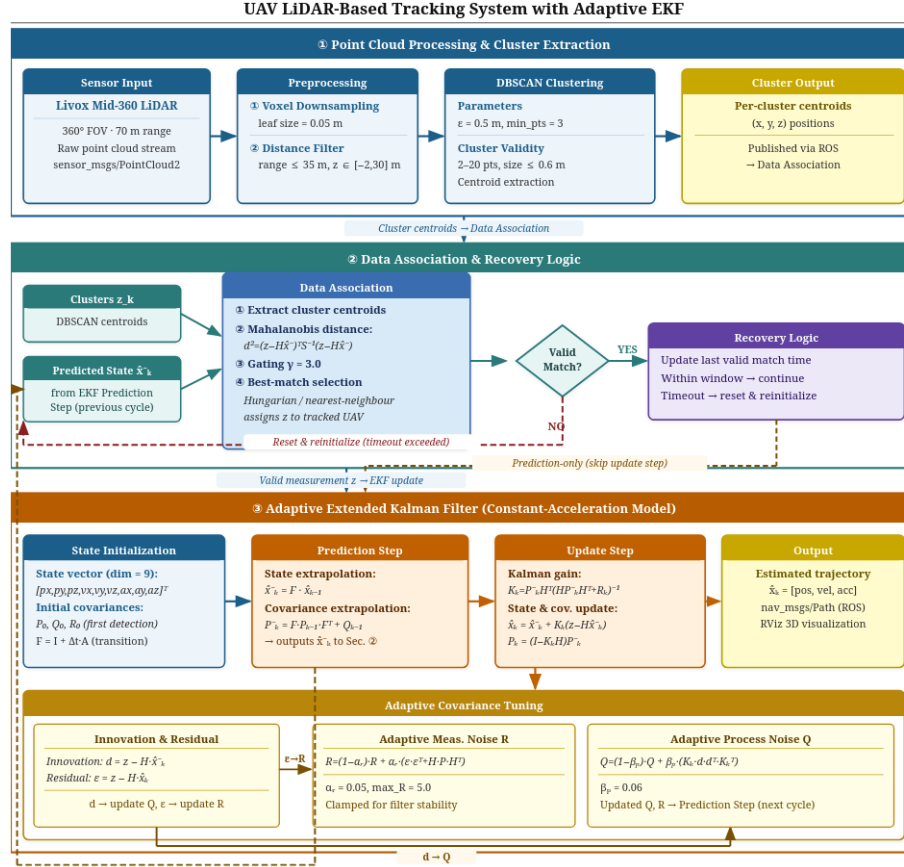


Fig. 1: Complete system architecture: LiDAR point cloud processing and cluster extraction (Stage I), data association and recovery logic (Stage II), and Adaptive EKF with online Q_k/R_k tuning (Stage III). The feedback arrow from the EKF predicted state \hat{x}_k to the association gate closes the estimation loop.

providing accurate 3D spatial information, LiDAR sensors enable reliable UAV detection even when visual data is compromised.

Early work by Razlaw et al. [12] mounted a Velodyne VLP-16 on a DJI Matrice 600 MAV and applied Euclidean clustering with a fixed-parameter Kalman filter to track small *ground-level* objects not other UAVs using fixed noise parameters. Dogru and Marques [11] advanced ground-based drone detection by combining probabilistic track-before-detect models with Bayesian filtering on a Velodyne VLP-16, although the method required substantial computational resources. Catalano et al. [10] further enhanced the accuracy of tracking in GNSS-denied settings by adaptively integrating 2–50 solid-state LiDAR scans with specialized Kalman filtering, though this was limited to field-based ground deployments; the word “adaptive” here refers to scan-count selection, not noise covariance estimation.

Researchers have also explored alternative LiDAR configurations to improve tracking performance. Gazdag et al. [13] mounted a Livox AVIA rosette-scanning LiDAR on a ground pan-tilt turret, combining particle filtering with OctoMap background subtraction for active tracking, though the bulky pan-tilt mechanism limits platform portability and noise parameters remain fixed. Sier et al. [14] demonstrated that reinterpreting LiDAR scans as panoramic images and applying YOLOv5 enables tracking-by-detection from a fixed ground platform. Abir et al. [6] studied point cloud characteristics of small UAVs using a static Livox Mid-40 array and proposed adaptive thresholding for detection, but without state estimation. Balla et al. [15] addressed the challenge of discriminating UAVs from birds in sparse point clouds using attention-based segmentation and CNN classification on a ground pan-tilt system, focusing on detection and classification only. Leuci et al. [3] demonstrated camera–LiDAR fusion in a heterogeneous UAV–UGV team but required multi-sensor calibration and fixed noise models. Chen et al. [16] used a 2D laser scanner on a quadrotor for collision-free trajectory *generation* in cluttered environments a navigation task rather than target tracking.

A structured comparison is provided in Table 1. Across all existing work, **no system** simultaneously achieves: (i) online adaptive noise covariance estimation (Q_k and R_k), (ii) UAV-to-UAV relative tracking from an airborne platform, and (iii) a non-repetitive scanning LiDAR on a payload-constrained platform.

Existing approaches typically rely on fixed noise parameters in their filtering frameworks, limiting adaptability to dynamic environments and variable data quality. Most systems focus on ground-based tracking or require specialised hardware not suitable for lightweight platforms. Critically, *no existing work* combines online adaptive noise covariance estimation with UAV-to-UAV relative tracking using a non-repetitive scanning LiDAR on a payload-constrained airborne platform.

Our approach differs by implementing an Adaptive Kalman Filter that responds to real-time variations in both UAV motion and measurement quality from non-repetitive scanning patterns. As shown in Fig. 1, our framework integrates point cloud processing, optimised clustering, track management, and adaptive noise estimation. By dynamically adjusting noise parameters based on innovation and residual statistics, our system mitigates tracking errors where measurement quality varies significantly. Comparative evaluations confirm superior accuracy, robustness, and target reacquisition performance in challenging conditions with rapid maneuvers and intermittent detections.

4 Methodology

We employ an adaptive Kalman filter (AKF) inspired by [17] that dynamically adjusts both noise covariances to overcome the inaccuracies of fixed-parameter filters under varying sensor conditions and dynamic motion. The framework integrates three components: (i) point cloud processing and detection, (ii) adaptive state estimation, and (iii) data association and occlusion handling.

Table 1: Representative LiDAR-Based UAV Tracking Approaches.

Approach	Configuration	Sensor	Core Method	Key Limitation
Dogru & Marques (2022) [11]	Ground → Drone	Velodyne VLP-16	Track-before-detect + Bayesian filter	High compute; fixed noise model
Catalano et al. (2023) [10]	Ground → Drone	Solid-state LiDAR	Multi-scan EKF (adaptive scan count only)	Ground-only; no noise adaptation
Gazdag et al. (2024) [13]	Pan-tilt → Drone	Livox AVIA (rosette)	Particle filter + background subtraction	Bulky pan-tilt; fixed noise model
Sier et al. (2023) [14]	Fixed ground → Drone	Ouster (LiDAR-image)	YOLOv5 tracking-by-detection	Fixed platform; ML inference cost
Leuci et al. (2024) [3]	UAV+UGV → Drone	Camera + LiDAR	Multi-sensor fusion + KF	Calibration burden; fixed noise
Chen et al. (2016) [16]	UAV (self-navigation)	2D laser + IMU	QP trajectory optimisation	Navigation only; no target tracking
Razlaw et al. (2019) [12]	MAV → Ground objects	Velodyne VLP-16	Euclidean clustering + KF (fixed)	Tracks ground targets; fixed noise
Abir et al. (2023) [6]	Ground → Drone	Livox Mid-40 (static)	Adaptive threshold detection	Detection only; no state estimation
Balla et al. (2024) [15]	Pan-tilt → Drone/Bird	Livox AVIA (rosette)	CNN classification + segmentation	Classification only; no tracking
Proposed (AEKF)	UAV → UAV	Livox 360 (non-rep.)	Adaptive EKF (Q_k, R_k) + DB-SCAN + recovery	First adaptive noise covariance tracker on airborne LiDAR platform

4.1 LiDAR Data Processing and Object Detection

This stage extracts potential drone targets from raw LiDAR point clouds through a three-step process (Algorithm 1).

Step 1 — Voxel Downsampling. The raw cloud $P = \{p_i\}_{i=1}^N$, $p_i \in \mathbb{R}^3$, is partitioned into cubic voxels of side $v = 0.05$ m; each non-empty voxel V_j is replaced by its centroid:

$$c_j = \frac{1}{|V_j|} \sum_{p_i \in V_j} p_i, \quad (1)$$

yielding the downsampled cloud P' .

Step 2 — Cylindrical ROI Filter. Points outside the flight envelope are discarded:

$$P_{\text{ROI}} = \{p \in P' \mid \sqrt{x^2 + y^2} < d_{\text{max}}, z_{\text{min}} < z < z_{\text{max}}\}, \quad (2)$$

with $d_{\text{max}} = 35$ m and altitude limits $[z_{\text{min}}, z_{\text{max}}]$ bounding the expected flight envelope.

Step 3 — DBSCAN Clustering. A point $p \in P_{\text{ROI}}$ is a *core point* [18] if

$$|\mathcal{N}_\epsilon(p)| \geq M_{\min}, \quad \mathcal{N}_\epsilon(p) = \{q \mid \|p-q\| \leq \epsilon\}. \quad (3)$$

Clusters $\mathcal{C} = \{C_1, \dots, C_K\}$ are maximal sets of density-connected points; unreachable points are noise. We use $\epsilon = 0.5$ m, $M_{\min} = 3$, tuned to the 1–4 points the Livox Mid-360 returns per scan on a DJI F550 at 10–35 m.

Cluster Characterisation and Candidate Validation. For each cluster C_k , centroid and sample covariance are:

$$\boldsymbol{\mu}_k = \frac{1}{|C_k|} \sum_{p \in C_k} p, \quad (4)$$

$$\boldsymbol{\Sigma}_k = \frac{1}{|C_k|-1} \sum_{p \in C_k} (p - \boldsymbol{\mu}_k)(p - \boldsymbol{\mu}_k)^T. \quad (5)$$

A cluster is a UAV candidate only if

$$2 \leq |C_k| \leq N_{\max}, \quad \max_i \lambda_i(\boldsymbol{\Sigma}_k) \leq \sigma_{\max}^2, \quad (6)$$

where $\lambda_i(\boldsymbol{\Sigma}_k)$ are eigenvalues of $\boldsymbol{\Sigma}_k$. This rejects single-point spurious returns and large extended objects. The surviving centroid $\boldsymbol{\mu}_k$ forms measurement \mathbf{z}_k .

```

Input: Raw cloud  $P$ ;
 $v=0.05$  m;;
 $d_{\max}=35$  m,  $z_{\min}$ ,  $z_{\max}$ ;
 $\epsilon=0.5$  m,  $M_{\min}=3$ ;
 $N_{\max}$ ,  $\sigma_{\max}$ 
Output: Candidate measurement  $\mathbf{z}_k$  (or  $\emptyset$  if none)
// Step 1 - Voxel downsampling (Eq. 1)
 $P' \leftarrow \{\text{centroid}(V_j) : V_j \subset P, V_j \neq \emptyset\}$ ;
// Step 2 - Cylindrical ROI filter (Eq. 2)
 $P_{\text{ROI}} \leftarrow \{p \in P' \mid \sqrt{x^2+y^2} < d_{\max}, z_{\min} < z < z_{\max}\}$ ;
// Step 3 - DBSCAN clustering (Eq. 3)
 $\mathcal{C} \leftarrow \text{DBSCAN}(P_{\text{ROI}}, \epsilon, M_{\min})$ ;
// Step 4 - Cluster validation (Eqs. 4-6)
for each  $C_k \in \mathcal{C}$  do
    Compute  $\boldsymbol{\mu}_k, \boldsymbol{\Sigma}_k$ ;
    if  $2 \leq |C_k| \leq N_{\max}$  and  $\max_i \lambda_i(\boldsymbol{\Sigma}_k) \leq \sigma_{\max}^2$  then
        | return  $\mathbf{z}_k = \boldsymbol{\mu}_k$ ;
    end
end
return  $\emptyset$ 
Algorithm 1: LiDAR Data Processing and Object Detection

```

4.2 Adaptive Kalman Filtering for UAV State Estimation

State Space Model. A constant-acceleration (CA) model captures agile flight dynamics. The nine-dimensional state is

$$\mathbf{x}_k = [p_x \ p_y \ p_z \ v_x \ v_y \ v_z \ a_x \ a_y \ a_z]^T, \quad (7)$$

with transition matrix $F \in \mathbb{R}^{9 \times 9}$ derived from CA kinematics at interval Δt :

$$F = \begin{bmatrix} I_3 & \Delta t I_3 & \frac{\Delta t^2}{2} I_3 \\ 0_3 & I_3 & \Delta t I_3 \\ 0_3 & 0_3 & I_3 \end{bmatrix}. \quad (8)$$

State evolution and LiDAR position measurement are:

$$\mathbf{x}_k = F \mathbf{x}_{k-1} + \mathbf{w}_k, \quad \mathbf{w}_k \sim \mathcal{N}(\mathbf{0}, Q_k), \quad (9)$$

$$\mathbf{z}_k = H \mathbf{x}_k + \mathbf{v}_k, \quad \mathbf{v}_k \sim \mathcal{N}(\mathbf{0}, R_k), \quad (10)$$

where $H = [I_{3 \times 3} \ 0_{3 \times 6}]$ selects position components.

Filter Equations. The filter cycles through prediction and update at each step k . *Prediction:*

$$\hat{\mathbf{x}}_k^- = F \hat{\mathbf{x}}_{k-1}^+, \quad (11)$$

$$P_k^- = F P_{k-1}^+ F^T + Q_k. \quad (12)$$

Update (given valid \mathbf{z}_k):

$$S_k = H P_k^- H^T + R_k, \quad (13)$$

$$K_k = P_k^- H^T S_k^{-1}, \quad (14)$$

$$\hat{\mathbf{x}}_k^+ = \hat{\mathbf{x}}_k^- + K_k (\mathbf{z}_k - H \hat{\mathbf{x}}_k^-), \quad (15)$$

$$P_k^+ = (I - K_k H) P_k^-. \quad (16)$$

Process Noise Adaptation. The innovation $\mathbf{d}_k = \mathbf{z}_k - H \hat{\mathbf{x}}_k^-$ grows when the target accelerates beyond the CA model's prediction. This drives

$$Q_k = \alpha Q_{k-1} + (1-\alpha) K_k \mathbf{d}_k \mathbf{d}_k^T K_k^T, \quad (17)$$

where $\alpha \in (0, 1)$ is a forgetting factor. A large $\|\mathbf{d}_k\|$ increases $Q_k \rightarrow$ larger P_k^- (12) \rightarrow larger K_k (14), making the filter more responsive; small innovations reduce Q_k , suppressing noise amplification during smooth flight.

Measurement Noise Adaptation. The post-update residual $\boldsymbol{\varepsilon}_k = \mathbf{z}_k - H \hat{\mathbf{x}}_k^+$ quantifies measurement quality. Elevated $\|\boldsymbol{\varepsilon}_k\|$ (e.g. when the target returns only 1–2 points) triggers

$$R_k = \beta R_{k-1} + (1-\beta) (\boldsymbol{\varepsilon}_k \boldsymbol{\varepsilon}_k^T + H P_k^- H^T), \quad (18)$$

where the $H P_k^- H^T$ term debiases the estimator by removing the prediction uncertainty contribution. Together, Eqs. (17) and (18) form a dual-channel self-tuning loop operating purely from observable statistics. Both Q_k and R_k remain positive semi-definite for all k by construction, guaranteeing numerical stability.

4.3 Data Association and Occlusion Handling

Mahalanobis Gating. A candidate \mathbf{z}_k is accepted only if

$$D_M^2 = (\mathbf{z}_k - H\hat{\mathbf{x}}_k^-)^T S_k^{-1} (\mathbf{z}_k - H\hat{\mathbf{x}}_k^-) < \tau, \quad (19)$$

where $\tau = \chi_{3,\gamma}^2$ (e.g. $\tau \approx 14.16$ for $\gamma = 0.997$). The ellipsoidal gate scales automatically with P_k^- and R_k : tighter when certain, wider after measurement gaps.

Occlusion and Reinitialization. When no measurement passes the gate, the filter propagates in prediction-only mode:

$$\hat{\mathbf{x}}_k^+ = \hat{\mathbf{x}}_k^-, \quad P_k^+ = P_k^-. \quad (20)$$

P_k^+ grows via (12), reflecting accumulating uncertainty while Q_k is frozen. After t_{occ} consecutive missed steps the track is reinitialized from the next valid cluster, bounding the prediction horizon and preventing the unbounded acceleration extrapolation that causes Fixed CA-KF divergence.

5 Experimental Results

A DJI F550 UAV with a Jetson Nano and Livox Mid-360 LiDAR served as the observer; a second DJI F550 with an Intel NUC acted as the freely maneuvering target. RTK positioning on both UAVs provided ground truth, synchronized and transformed to a common reference frame (Fig. 2).



Fig. 2: Flight test scenario showing both UAVs in operation. The observer UAV (left) is equipped with a Livox Mid-360 LiDAR, while the target UAV (right) performs randomized maneuvers for tracking evaluation across diverse ranges and orientations.

5.1 LiDAR Processing Pipeline

Figure 3 shows the three pipeline stages on a representative frame: **(left)** voxel-downsampled cloud; **(center)** DBSCAN-clustered segments with annotated centroid and covariance σ ; **(right)** selected drone candidate (black cross) after Mahalanobis gating. In ambiguous cases (birds, foliage producing drone-like returns), the size-and-extent gate (Eq. 6) and the Mahalanobis gate jointly reject outliers.

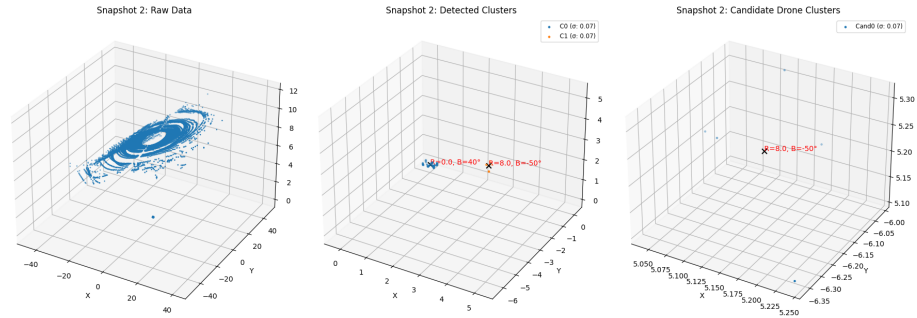


Fig. 3: Sequential stages of the LiDAR preprocessing and target-detection pipeline. From left to right: raw downsampled point cloud, Euclidean clustering with cluster statistics, and final drone candidate selection after geometric validation and Mahalanobis gating.

5.2 Results

To evaluate different filtering strategies we implemented three approaches:

1. **Fixed CA-KF**: A standard constant acceleration Kalman filter with fixed (non-adaptive) noise covariance matrices.
2. **Particle Filter (PF)**: A non-parametric approach using 2000 particles with systematic resampling.
3. **Adaptive CA-EKF (CAEKF)**: Our proposed approach, which uses the same constant acceleration model as the Fixed CA-KF but incorporates adaptive noise estimation and recovery logic.

Qualitative examination of trajectory estimates (Fig. 4) reveals different performance characteristics for each filtering approach. The CAEKF (red line) demonstrates exceptional tracking fidelity, maintaining consistent proximity to the RTK reference (black line) throughout the flight while producing a remarkably smooth trajectory with minimal lag or overshoot even during aggressive maneuvers.

By contrast, the Fixed CA-KF (green line) exhibits alarming periodic divergence reaching up to 50 m from ground truth at timestamps of approximately 480 s, 500 s, and 540 s. These divergences occur precisely during periods when the target UAV moved beyond the LiDAR’s effective range or became too small for reliable detection during fast horizontal sweeps. Without adaptive covariance tuning and track recovery, the fixed filter extrapolates the trajectory indefinitely using the last known acceleration, leading to catastrophic divergence that renders it unsuitable for high-agility UAV tracking.

The Particle Filter (yellow line) delivers intermediate performance, avoiding the catastrophic divergence of the Fixed CA-KF but exhibiting persistent jitter and reduced trajectory smoothness, particularly on the Y-axis between 520–540 s. This is consistent with well-known sample impoverishment during rapid state transitions, despite our implementation using 2000 particles.

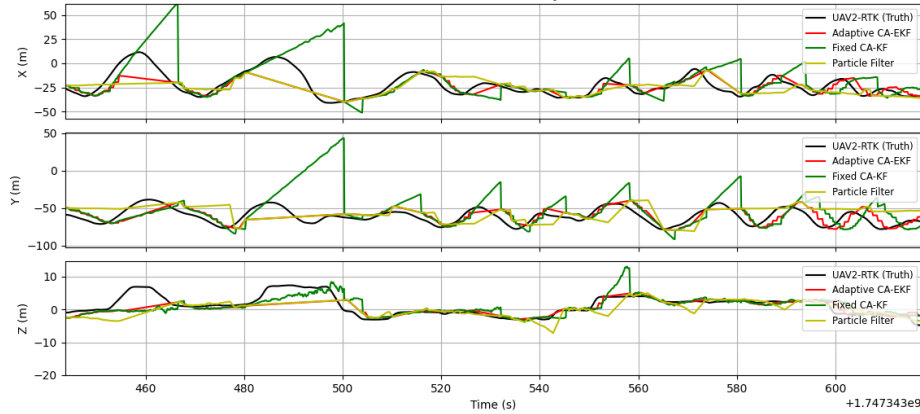


Fig. 4: Time-series comparison of UAV position along X, Y, and Z axes. RTK ground truth (black), Adaptive CA-EKF / CAEKF (red), Fixed CA-KF (green), and Particle Filter (yellow). The CAEKF maintains high tracking fidelity, while the Fixed CA-KF diverges during measurement gaps ($t \approx 480$ s, 500 s, 540 s) and the Particle Filter shows increased jitter during dynamic maneuvers.

Table 2 presents a detailed comparison of RMSE and computational metrics. The CAEKF achieves the lowest 3D RMSE (2.8 m), representing a **49.1%** reduction over the Particle Filter (5.5 m) and **78.5%** over the Fixed CA-KF (13.0 m), with X and Y RMSE of 3.0 m and 4.0 m versus 6.0/8.0 m (PF) and 15.0/20.0 m (Fixed CA-KF).

Table 2: Tracking accuracy and computational metrics on Jetson Nano under aggressive-maneuver flight. † Peak values elevated only during transient adaptation bursts, within four-core capacity. ‡ Lower valid-measurement rate reflects stricter adaptive gating a design strength, not a limitation.

Metric (Unit)	Fixed CA-KF	Particle Filter	CAEKF (Ours)
<i>(A) Tracking Accuracy RTK ground truth</i>			
RMSE _X (m)	15.0	6.0	3.0
RMSE _Y (m)	20.0	8.0	4.0
RMSE _Z (m)	4.0	2.5	1.5
RMSE _{3D} (m)	13.0	5.5	2.8
<i>(B) Computational Performance Jetson Nano (4-core ARM)</i>			
Avg. CPU (%)	106.4	0.99	106.5
Total Runtime (s)	178.9	179.1	174.8
Avg. Proc. Time (ms)	108.5	101.3	103.8
<i>(C) Filter Behaviour</i>			
Valid Measurements (%) [‡]	14.7	15.8	8.5
Callback Rate (Hz)	8.5	9.2	9.3

A critical consideration is computational efficiency. The CAEKF maintains an average processing time of 103.8ms per update lower than the Fixed CA-

KF’s 108.5 ms and only marginally above the Particle Filter’s 101.3 ms while achieving the highest callback rate (9.3 Hz) and comparable average CPU usage (106.5%). The lower valid-measurement acceptance rate (8.5% vs. 14.7% and 15.8%) reflects stricter Mahalanobis gating enabled by adaptive R_k , focusing the filter on high-confidence LiDAR returns. Whereas the Fixed CA-KF diverges catastrophically in prediction-only mode, the CAEKF dynamically increases Q_k to bound extrapolation uncertainty until sensor updates resume.

6 Conclusion

This paper presented a LiDAR-based UAV tracking framework that uses an Adaptive Extended Kalman Filter to improve state estimation in dynamic, uncertain environments. Unlike baseline methods that rely on fixed noise covariance parameters, our approach adjusts both process and measurement noise in real time based on innovation and residual statistics. This adaptive strategy improves tracking precision under a wide range of conditions, as confirmed by real-world flight experiments that demonstrated improved accuracy, robustness to noise variations, and responsiveness to rapid UAV maneuvers.

A central feature of our framework is the use of a constant acceleration motion model, which offers increased flexibility over traditional constant-velocity models when tracking UAVs performing nonlinear maneuvers. By incorporating acceleration into the model, the filter is better able to capture sudden changes in speed and direction, an essential quality for real-world applications where abrupt movements are common. Our experimental results show that the adaptive filter significantly reduces estimation errors (RMSE_{3D} of 2.8 m vs. 5.5 m and 13.0 m for competing methods), prevents divergence, and maintains stable trajectories compared to standard filtering techniques. The integration of Mahalanobis distance-based gating enhances measurement association, while our adaptive noise regulation minimizes tracking errors and avoids overconfidence in uncertain measurements. Additionally, our track management module successfully maintains continuous tracking during temporary target loss, effectively addressing challenges from sparse LiDAR returns and occlusions.

Future work will extend the framework to multi-target tracking in cluttered environments, improving data association, reducing false positives, and optimizing computational efficiency. We also plan to investigate the integration of deep learning-based detection with adaptive filtering to further enhance robustness in complex aerial operations.

In conclusion, our findings demonstrate the promise of adaptive Kalman filtering for UAV trajectory estimation and its potential to support scalable, autonomous aerial systems, particularly in GPS-denied or otherwise challenging environments.

Acknowledgments

This work was supported by the Aero.Next project (PRR - C645727867-00000066) and LARSyS funding (DOI: 10.54499/LA/P/0083/2020, 10.54499/UIDP/50009/2020 and 10.54499/UIDB/50009/2020).

References

- [1] Shi, X., Yang, C., Xie, J., Liang, C., Chen, J.: Anti-Drone System with Multiple Surveillance Technologies: Architecture, Implementation, and Challenges. *IEEE Communications Magazine* **56**(4), 68–74 (2018). <https://doi.org/10.1109/MCOM.2018.1700430>
- [2] Wang, B., Li, Q., Mao, Q., Wang, J., Chen, C.L.P., Shangguan, A., Zhang, H.: A Survey on Vision-Based Anti Unmanned Aerial Vehicles Methods. *Drones* **8**(9), 518 (2024). <https://doi.org/10.3390/drones8090518>
- [3] Leuci, C., Dogru, S., Marques, L.: Camera Lidar Fusion for Unmanned Aerial Vehicle Detection. In: 2024 7th Iberian Robotics Conference (ROBOT), pp. 1–6 (2024). <https://doi.org/10.1109/ROBOT61475.2024.10796952>
- [4] Zhu, P., Wen, L., Du, D., Bian, X., Fan, H., Hu, Q., Ling, H.: Detection and Tracking Meet Drones Challenge. *IEEE Transactions on Pattern Analysis and Machine Intelligence* **44**(11), 7380–7399 (2022). <https://doi.org/10.1109/TPAMI.2021.3119563>
- [5] Vrba, M., Heřt, D., Saska, M.: Onboard Marker-Less Detection and Localization of Non-Cooperating Drones for Their Safe Interception by an Autonomous Aerial System. *IEEE Robotics and Automation Letters* **4**(4), 3402–3409 (2019)
- [6] Abir, T.A., Kuantama, E., Han, R., Dawes, J., Mildren, R., Nguyen, P.: Towards Robust Lidar-based 3D Detection and Tracking of UAVs. In: Proceedings of the Ninth Workshop on Micro Aerial Vehicle Networks, Systems, and Applications (DroNet '23), pp. 1–7. ACM, New York (2023). <https://doi.org/10.1145/3597060.3597236>
- [7] Hammer, M., Hebel, M., Laurenzis, M., Arens, M.: Lidar-based detection and tracking of small UAVs. In: *Security + Defence* (2018)
- [8] Nie, C., Ju, Z., Sun, Z., Zhang, H.: 3D Object Detection and Tracking Based on Lidar-Camera Fusion and IMM-UKF Algorithm Towards Highway Driving. *IEEE Transactions on Emerging Topics in Computational Intelligence* **7**(4), 1242–1252 (2023). <https://doi.org/10.1109/TETCI.2023.3259441>
- [9] Livox Technology Ltd: Livox Mid-360 User Manual. Livox Technology Official Documentation (2023). <https://www.livoxtech.com/mid-360>
- [10] Catalano, I., Sier, H., Yu, X., Peña Queralta, J., Westerlund, T.: UAV Tracking with Solid-State Lidars: Dynamic Multi-Frequency Scan Integration. arXiv preprint arXiv:2304.12125 (2023). <https://doi.org/10.48550/arXiv.2304.12125>

- [11] Dogru, S., Marques, L.: Drone Detection Using Sparse Lidar Measurements. *IEEE Robotics and Automation Letters* **7**(2), 3062–3069 (2022). <https://doi.org/10.1109/LRA.2022.3145498>
- [12] Razlaw, J., Quenzel, J., Behnke, S.: Detection and Tracking of Small Objects in Sparse 3D Laser Range Data. In: 2019 International Conference on Robotics and Automation (ICRA), pp. 2967–2973 (2019)
- [13] Gazdag, S., Moller, T., Keszler, A., Majdik, A.: Detection and Tracking of MAVs Using a Rosette Scanning Pattern LiDAR. arXiv:2408.08555 (2024)
- [14] Sier, H., Yu, X., Catalano, I., Queralta, J.P., Zou, Z., Westerlund, T.: UAV Tracking with Lidar as a Camera Sensor in GNSS-Denied Environments. In: 2023 International Conference on Localization and GNSS (ICL-GNSS), pp. 1–7 (2023). <https://doi.org/10.1109/ICL-GNSS57829.2023.10148919>
- [15] Balla, K., Keszler, A., Gazdag, S., Szirányi, T., Majdik, A.L.: Detection and Classification of Small-sized UAVs and Birds in Sparse LiDAR Point Cloud. In: 2024 IEEE International Symposium on Safety Security Rescue Robotics (SSRR), pp. 172–177 (2024). <https://doi.org/10.1109/SSRR62954.2024.10770035>
- [16] Chen, J., Liu, T., Shen, S.: Online generation of collision-free trajectories for quadrotor flight in unknown cluttered environments. In: 2016 IEEE International Conference on Robotics and Automation (ICRA), pp. 1476–1483 (2016). <https://doi.org/10.1109/ICRA.2016.7487283>
- [17] Akhlaghi, S., Zhou, N., Huang, Z.: Adaptive adjustment of noise covariance in Kalman filter for dynamic state estimation. In: 2017 IEEE Power & Energy Society General Meeting, pp. 1–5 (2017). <https://doi.org/10.1109/PESGM.2017.8273755>
- [18] Ester, M., Kriegel, H.-P., Sander, J., Xu, X.: A density-based algorithm for discovering clusters in large spatial databases with noise. In: Proceedings of the 2nd International Conference on Knowledge Discovery and Data Mining (KDD-96), pp. 226–231 (1996)